A Web-Controlled, Modular 3D-Printed Exoskeleton for Upper Limb Stroke Recovery

Crina Bărbieru^{©a} and Isabela Drămnesc^{©b}

Department of Computer Science, West University of Timişoara, Romania

Keywords: Robotic Hand Exoskeleton, Stroke Rehabilitation, 3D-Printed Exoskeleton, Remote Monitoring, Web-Based

Rehabilitation Platform.

Abstract: Stroke survivors often experience partial or complete loss of hand function, significantly affecting their ability

to perform everyday tasks. Current rehabilitation methods can be resource intensive and require significant human intervention. This paper aims to develop a portable, modular, 3D-printed robotic hand exoskeleton that provides targeted repetitive exercises designed to enhance motor recovery. This exoskeleton is controlled via a web application, which includes progress-tracking functionalities for both patients and physical therapists, enabling remote monitoring. Preliminary testing was conducted with one patient to evaluate the usability and efficacy of the device. Feedback was collected from a physical therapist to assess the feasibility of the exoskeleton. The proposed system offers a scalable, cost-effective solution for post-stroke hand rehabilitation.

Further studies with larger cohorts are needed to validate efficacy.

1 INTRODUCTION

Stroke is one of the leading global causes of death and long-term disability, with nearly 12 million new cases every year (Feigin et al., 2025). Approximately 25.3% of patients develop post-stroke spasticity (Zeng et al., 2021), a condition in which muscle stiffness and abnormal muscle contractions affect movement, limiting their ability to perform daily tasks and regain independence.

The development of innovative therapeutic tools, such as robotic exoskeletons, holds promise for improving the rehabilitation process, particularly for those with limited mobility due to spasticity. Some studies found robot-assisted therapy in acute and subacute stroke patients more effective than traditional therapy (Masiero et al., 2007; Sale et al., 2014; Takahashi et al., 2016), although others found no significant differences between the two approaches if exercises were performed at a similar intensity (Kahn et al., 2006; Hesse et al., 2014).

In the last three decades, a wide range of upperlimb robotic exoskeletons have been developed for patients to perform independent and repeatable exercises remotely, allowing for a more personalized ap-

^a https://orcid.org/0009-0004-1794-6510

b https://orcid.org/0000-0003-4686-2864

proach to rehabilitation. However, many existing systems rely on minimal control interfaces, with little capability for progress tracking or therapist supervision. The aim of this paper is to address some of the gaps in existing solutions and design a portable, 3D-printed, modular exoskeleton controlled via a web application, enhancing the patient's rehabilitation experience and streamlining the progress supervision process.

2 RELATED WORK

Finding a balance between design simplicity and portability constitutes a significant challenge when designing a robotic hand exoskeleton. We can distinguish a category of exoskeletons that actuate the fingers via cable systems placed on the palmar side of the hand. While it is relatively straightforward, this approach can prevent patients from fully sensing and grasping objects during rehabilitation exercises. The device described in (Selvaraj Mercyshalinie et al., 2023) uses fishing lines attached to distal interphalangeal (DIP) joint hooks and guided through metacarpophalangeal (MCP) joint hooks. The modular exoskeleton developed by (Chirinos and Vela, 2021) assists with the flexion and extension of the thumb, index, and middle fingers using a pulley connected to a direct current (DC) motor. Teflon tubes guiding the wires allow for better object-grasping capabilities, although they still remain limited.

This issue can be solved by placing cables on the sides of the fingers, as can be observed in (Chiri et al., 2009). Extension is actively achieved via Bowden cables pulled by a slider connected to the DC motor. DC motors are commonly used in robotic applications due to their precise control and compact size. Their rotational torque can be adapted to simulate the movement generated by a linear actuator, which is the mechanism leveraged by (Chiri et al., 2009). Flexion is achieved passively, with cables attached to linear compression springs.

Some of the existing solutions flex the fingers by pushing rather than pulling them, allowing the palmar side of the hand to remain free. The portability of devices in this category is influenced by the choice of hardware components. In (Wang et al., 2020) the palm is positioned in an upward position and braces support it to prevent fatigue. The system flexes one finger at a time via pneumatic muscles attached to plates and wheels of different radii. This setup significantly limits the range of rehabilitation exercises which can be performed. (Ho et al., 2011) uses a linear actuator and a dual arch guide mechanism to actuate the MCP and proximal interphalangeal (PIP) joints. Electromyography (EMG) sensors are integrated to detect movement intent and a wireless control unit allows the therapist to choose from different training modes. The exoskeleton described in (Sandison et al., 2020) achieves a 90° range of motion (ROM) at the MP and 100° at the PIP. The elastic distal segment is user dependent and can be avoided to achieve tactile sensation when grasping objects.

The integration of 3D-printing technology in robotic exoskeletons has enabled more innovative, customizable designs and has lead to the development of new actuation mechanisms. (Yap et al., 2015) uses 3D-printed molds to create accordion-like, elastomer actuators. Actuators in (Ridremont et al., 2024) are pressurized to flex the joints and vacuumed to extend them, while those in (Yap et al., 2017) use the opposite mechanism. Other devices (Fiorilla et al., 2009; Sandison et al., 2020; Selvaraj Mercyshalinie et al., 2023) use 3D-printed parts as components of the exoskeleton to lower the cost, reduce the weight, and more easily adapt the exoskeleton to diverse patient needs

Although most robotic exoskeletons are controlled via hardware components, some implement mobile or Web applications to personalize rehabilitation sessions and improve user experience. In (Fiorilla et al., 2009), the application developed in Microsoft Visual C++ and National Instruments

LabViewTM communicates with the robot's controller, reads the input from sensors and encoders to reconstruct the MCP angle and monitors the device during rehabilitation exercises. The Android mobile application in (Selvaraj Mercyshalinie et al., 2023) contains buttons for each individual finger. Flexion is done gradually, in three stages, and the fingers are relaxed by pressing dedicated buttons.

3 EXOSKELETON DESIGN

The proposed solution utilizes the advantages of 3D-printed components to design a modular robotic exoskeleton. The current system is comprised of a single-finger module, with the possibility to connect multiple such modules to achieve a full-hand exoskeleton.

3.1 Hardware Components

The robotic exoskeleton is controlled by an Arduino Nano ESP32 board, chosen for its integrated Wi-Fi, enabling communication with the web-based client interface. Thus, users are able to remotely select exercise modes and intensity.

Figure 1 illustrates the wiring configuration of the exoskeleton's electronic components. The MG90S servomotor interfaces with the Arduino via the D9 digital pin, utilizing Pulse Width Modulation (PWM) for precise control.

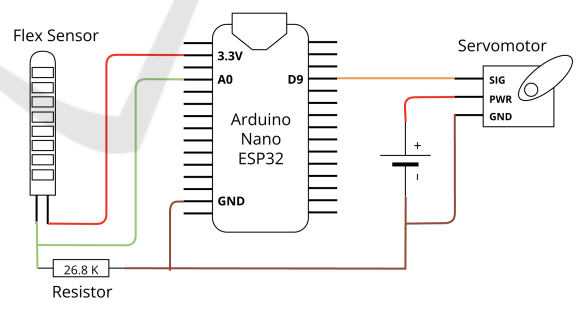


Figure 1: Circuit Diagram of the System.

Due to the Arduino Nano ESP32's 3.3V logic level, the 5V servomotor cannot be directly powered by the board. Instead, an external power source is employed, consisting of a power bank module. This module supplies 5V at 2A, sufficient to drive multiple servomotors if needed. To ensure a common reference voltage, the grounds of the Arduino, servomotor, and power bank are interconnected.

The flex sensor input is measured using a voltage divider circuit, a configuration which reduces the

voltage to a lower value while maintaining constant current flowing through the resistors. In this setup, the input voltage spans the entire resistor network. The output voltage is measured from the junction between two resistors, with its magnitude dictated by their resistance ratio. The flex sensor has a nominal resistance of $10K\Omega(\pm 30\%)$, and when paired with a $26.8K\Omega$ fixed resistor, the resulting voltage division ensures analog readings remain below the midpoint of the Arduino's 12-bit analog to digital converter (ADC) range (2047). The sensor is powered directly from the Arduino's 3.3V pin, which serves as the voltage divider's supply source, ensuring compatibility with the board's analog input range.

3.2 3D-Printed Components

The components of the exoskeleton are designed using Autodesk Tinkercad (Autodesk Inc., 2025), a web-based computer-aided design (CAD) platform that simplifies 3D modeling through an intuitive, primitive-based approach. CraftWare Pro is used to slice the components with fine layer resolution, which are then printed using the Craftbot Flow 3D printer. The distal and metacarpal components use a thermoplastic polyurethane (TPU) 95A filament. This semi-flexible, rubber-like material allows the exoskeleton to fit more comfortably on different finger sizes. The other components, involved in the actuation mechanism, are printed using a polylactic acid (PLA) filament. This material is selected for its strength, as it needs to withstand repeated mechanical stress.

The fingertip interface (Figure 2a) positioned on the distal phalanx, supports the attachment of two guide rods, which are designed to follow an arched channel. The metacarpal component (Figure 2b) provides structural support and serves as the mounting point for the arched component. Two tubular extensions on either side of mounting channel guide the wires used by the actuation mechanism.



Figure 2: 3D Models of Exoskeleton Components.

(b) Metacarpal Element.

(a) Distal Element.

The arched component (Figure 3) guides the rodshaped components (Figure 4) placed laterally, which slide and convert the curved trajectory into a controlled flexion movement. This movement simultaneously bends the DIP and PIP joints, mimicking the natural movement of a finger.



Figure 3: 3D Model of Arched Component.



Figure 4: 3D Model of Rod-Shaped Component.

3.3 Actuation Mechanism

Actuation is achieved via a system of wires attached to a servomotor. A non-elastic wire is attached to the rod-shaped components, passes through the guide components mounted distally on the arch component and then through the guides integrated into the metacarpal component before terminating at the servomotor head.

During flexion, the servomotor's torque is transformed into the linear movement of the rods along the arched trajectory, as shown in Figure 5. Due to pulley-like elements guiding the non-elastic wire at the distal end of the arched component, the rotational movement of the servomotor head leads to a translational movement of the rods along the arched trajectory. The finger extension mechanism is achieved passively, through an elastic wire positioned between the proximal end of the arched element and the extremities of the rods. While the servomotor releases tension on the wires, the elastic wire provides the force necessary to pull back the rods and bring them into their initial position.

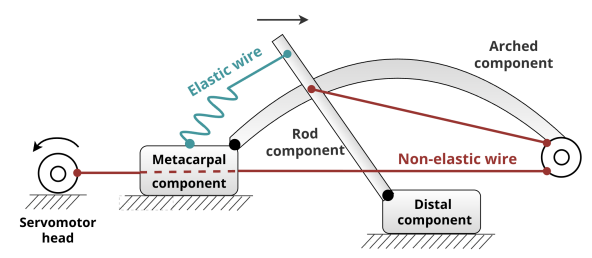
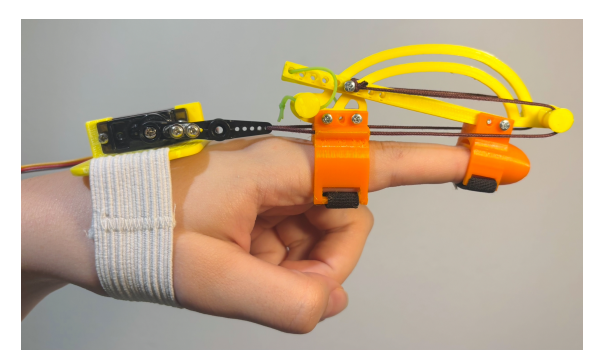


Figure 5: Kinematic Diagram of the System.

Figures 6a and 6b showcase the position of the finger when the exoskeleton assists with extension, and flexion respectively.



(a) Exoskeleton-Assisted Extension.



(b) Exoskeleton-Assisted Flexion.Figure 6: Finger Position During Exoskeleton-Assisted Exercises.

3.4 Sensors

The distal and metacarpal components of the exoskeleton have slots designed to accommodate the movement of the flex sensor during finger flexion and extension. The sensor is secured at the metacarpal component and passes freely through the fingertip's slot. This allows it to slide slightly as the distance between the two components increases when the finger is bent and decreases when the finger is fully extended.

When measuring the movement of the finger, the system first establishes a baseline reading with the finger fully extended. In this situation, the resistance of the flex sensor is minimum, while the voltage reaches its maximum value. During flexion, the resistance of the flex sensor increases, causing a proportional voltage drop. The system thus captures the combined bend of the DIP and PIP joints by tracking the voltage change.

4 SOFTWARE DESIGN

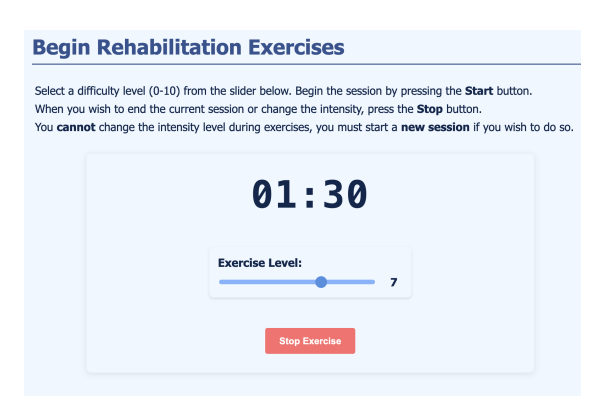
The robotic hand exoskeleton is controlled via a web application, which communicates with the robot us-

ing the controller's Wi-Fi module. The web application serves two distinct user roles: patients and supervisors. An intuitive and responsive interface improves the patient's experience, which not only serves as the control interface for the exoskeleton, but as a tool for recording exercise sessions and tracking progress. Furthermore, physical therapists are able to monitor the activity of their patients, essential for the safety and efficacy of remote rehabilitation.

The Client Layer is built with React, serving as the user interface patients and supervisors interact with. The Application Layer is a Spring Boot application, enforcing role-based access via Spring Security. Additionally, sensitive information, such as user passwords, is encrypted through BCrypt hashing. For persistent data storage, the system employs MySQL as its relational database management system. The relational model is suitable for the structured nature of the application's data, including user accounts and information related to exercise sessions.

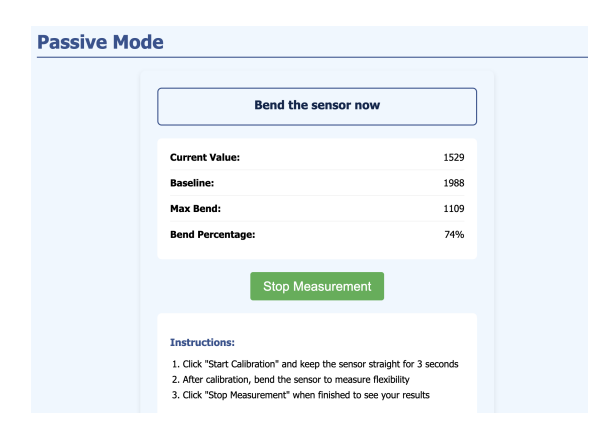
The patient Graphical User Interface (GUI) provides a control interface in the Active Exercises screen (Figure 7a), where they are able to select the level of intensity on a 1-10 scale and perform exoskeletonassisted, repeated movements. Level 1 represent a slight movement of the exoskeleton, and corresponds to a 18° rotation of the servomotor head, while level 10 ensures full exoskeleton movement and a 180° servomotor head rotation. In Passive Mode (Figure 7b), the patient attempts independent flexion and the application screen displays the flex sensor input as a percentage of the total range of movement of the DIP and PIP joints. All robot-assisted or passive sessions are recorded automatically and displayed in the Patient Progress component (Figure 7c). Patients view statistics related to their rehabilitation journey, such as the number of assisted exercise sessions completed in the current week, and a calendar containing both assisted and passive sessions.

Supervisors have a similar view over their patients' progress in the *Supervisor Progress* screen (Figure 7d), where the same data is aggregated and shown in the form of patient progress cards. The progress cards contain metrics about the patients medical information, such as: the number of days since the stroke occurred, the number of days in rehabilitation, and exercise sessions, like the number of sessions in the current week and average session duration. Furthermore, for better data visualization, the cards contain a similar calendar to that of the patients, but with exercise sessions and passive mode data summarized.



(a) Active Exercises Screen.





(b) Passive Mode Screen.

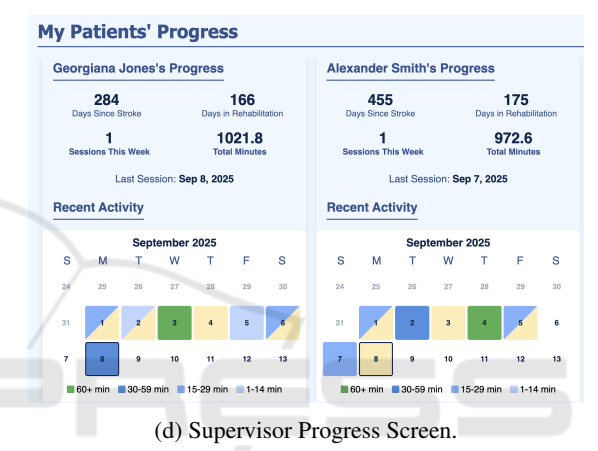


Figure 7: GUI Screens of the Web Application.

5 EXPERIMENTS AND RESULTS

The finger joint angles were analyzed using a custom Python script that combines computer vision tracking with geometric angle calculations. The OpenCV library is used to load a side-view recording capturing one full flexion movement of the exoskeleton. Three joint locations (MCP, PIP, DIP) and an additional point representing the finger tip (TIP) are manually selected on the first video frame. This is used for joint angle calculation, by applying the scalar product formula:

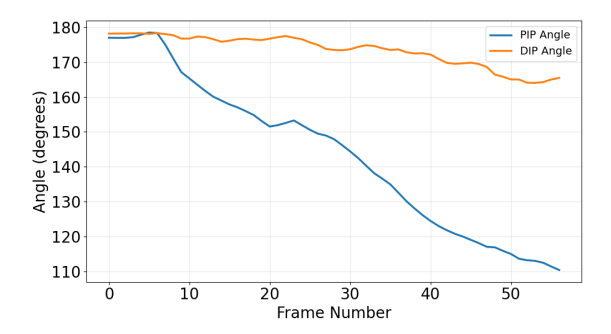
$$\theta_{PIP} = \cos^{-1} \left(\frac{(\mathbf{PIP} - \mathbf{MCP}) \cdot (\mathbf{DIP} - \mathbf{PIP})}{|\mathbf{PIP} - \mathbf{MCP}| \cdot |\mathbf{DIP} - \mathbf{PIP}|} \right) \quad (1)$$

$$\theta_{DIP} = \cos^{-1} \left(\frac{(\mathbf{DIP} - \mathbf{PIP}) \cdot (\mathbf{TIP} - \mathbf{DIP})}{|\mathbf{DIP} - \mathbf{PIP}| \cdot |\mathbf{TIP} - \mathbf{DIP}|} \right) \quad (2)$$

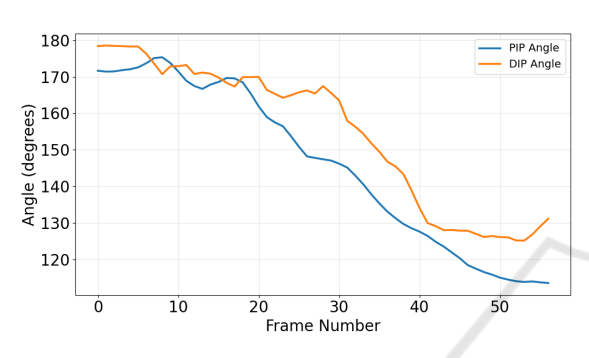
Initially, we attempted to automate joint detection and angle computation entirely through the CSRT algorithm (Channel and Spatial Reliability Tracking) OpenCV. However, due to interference from the exoskeleton's distal component, the TIP point could not be accurately identified, leading to incorrect DIP angle calculations (Figure 8a). To resolve this, we modified the program to allow periodic manual corrections, allowing us to reselect joint positions at fixed intervals. We tested three different scenarios, manually positioning the MCP, PIP, DIP and TIP points every 5, 8, and 10 frames respectively, to balance tracking accuracy with manual intervention.

The results revealed that the PIP joint reached a maximum angle of 110–115 degrees, corresponding to a flexion of 65–70 degrees from full extension. The DIP joint reached a peak flexion of approximately 65 degrees, although this decreased slightly to around 60 degrees towards the end of the movement. To ensure robustness, we applied a smoothing filter (3-frame moving average) to the raw angle data, thus filtering out noise and tracking errors between manual corrections. To contextualize our results, we consulted a physical therapist¹ with experience in the field of hand rehabilitation. We learned that similar

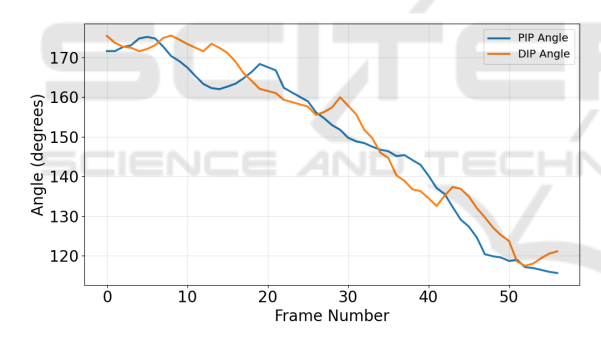
¹The physical therapist consented to the use of their feedback in this paper.



(a) Automatic Detection.



(b) 5-frame Correction.



(c) 8-frame Correction.

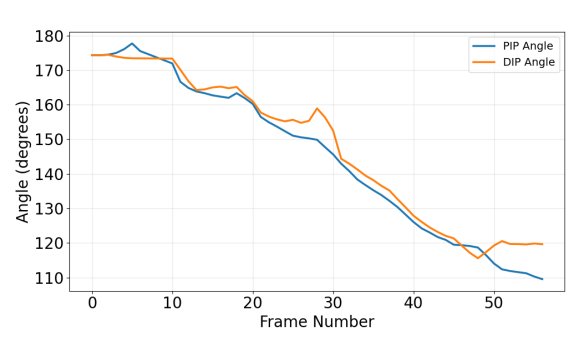


Figure 8: Experiment Results: PIP and DIP Angles During

(d) 10-frame Correction.

Exoskeleton-Assisted Flexion.

robotic technologies, particularly pneumatic-actuated gloves, tend to lose precision after 3–4 weeks as materials stretch and deform, limiting their clinical utility. While our 3D-printed PLA exoskeleton takes a different approach, similar wear-and-tear issues might eventually emerge with prolonged use. Since PLA isn't commonly used in clinical exoskeletons, or its use is limited and does not constitute a significant proportion of exoskeleton components, durability studies should be conducted to evaluate the performance of

We conducted additional experiments to measure the load on the elastic component of the exoskeleton. which not only assists in passive extension, but influences the flexion mechanism as an opposing force to the one generated by the torque of the servomotor. In this scenario, the chosen elastic component was latex wire with a diameter of 1 millimeter and $\approx 700\%$ elasticity. The exoskeleton was tested with a dynamometer to record applied forces. We measured that a force of about 0.8N was required to stretch the wire efficiently to enable full exoskeleton movement. The MG90S servomotor has a 1.8kg/cm stall torque at 4.8V. The non-elastic wire is fixed at 4cm from the servomotor shaft, therefore a maximum force of $\approx 4.4N$ can be applied before the servomotor stalls, in ideal conditions. Additional factors such as resistance from the elastic wire and the finger, friction between exoskeleton components and voltage drops could provide an explanation for the need of patient intervention when performing exoskeleton-assisted rehabilitation exercises, as the servomotor is not able to generate enough force for passive finger flexion. This is beneficial in situations where patient intervention is required during rehabilitation exercises, and the degree of intervention can be increased by choosing a thicker, less elastic wire.

Furthermore, we conducted preliminary testing with a patient² (Figure 9), who reported that the device was comfortable and lightweight.

Although we originally designed and tested the device for the index finger, the patient required rehabilitation for the little and ring fingers. This demonstrates an advantage of the modular exoskeleton, as it can be adapted and reused based on patient needs. During assisted flexion trials, the exoskeleton demonstrated measurable improvement, although the ROM was constrained by the patient's capability to initiate movement. The device augmented flexion by a small but consistent margin beyond the patient's independent effort, suggesting its potential as a training aid for motor recovery.

²The patient consented to the use of their feedback and photo in this paper.



Figure 9: Patient During Preliminary Testing.

A demonstration video showcasing the main features of our developed system can be accessed at https://youtu.be/LA84F36UVH4.

6 CONCLUSIONS AND FUTURE WORK

The developed system successfully integrates a 3D-printed finger exoskeleton with a web-based control interface. Similarly to (Chiri et al., 2009), it is a modular exoskeleton that uses active and passive mechanisms to flex and extend the fingers, though inverted (passive flexion and active extension). Where their design uses a system of 6 pulleys, 2 for each joint, the device described in this paper achieves simultaneous DIP and PIP flexion and extension via a set of servomotor-driven cables. This improvement reduces mechanical complexity while maintaining a comparable range of motion.

The arched trajectory mechanism is similar to that developed by (Ho et al., 2011), but with some optimization. The linear actuators are replaced with a servomotor cable system. (Ho et al., 2011) design features two arched components for the PIP and MCP joints, while this exoskeleton employs a single arch to simultaneously guide PIP and DIP movements.

Furthermore, 3D-printed PLA and TPU components increase portability and allow adjustments to accommodate a wider range of hand proportions. However, a key trade-off remains: the design's ability to withstand repetitive mechanical forces and maintain efficiency is uncertain and requires further testing.

The web application developed in this paper is an important improvement to previous systems. In addition to exoskeleton control and sensor feedback, it enhances the user's experience by providing relevant metrics related to the recovery process. Furthermore, it streamlines the supervision process and it offers a web interface for physical therapists to monitor their patients' activity.

While the current finger module demonstrates the system's core functionality, several improvements could be made to enhance its clinical utility.

The cable-driven actuation system presents limitations, as wire tension must be constantly maintained, requiring fixed-length cables or patient-specific adjustments. Transitioning to an alternative actuation mechanism would improve adaptability and reduce maintenance demands. Furthermore, incorporating MCP joint support would enable comprehensive finger rehabilitation, which is essential for restoring grasping functionality.

Expanding the exoskeleton to accommodate multiple fingers would be a critical step towards a full-hand exoskeleton. The expansion would require hardware upgrades, including a servomotor shield to supplement the Arduino Nano's limited I/O capabilities.

Before widespread adoption, the exoskeleton efficacy must be evaluated through controlled trials with stroke patients. These studies should quantitatively measure progress, and comparing the recovery rates in exoskeleton-assisted patients versus patients who undergo traditional therapy regimens. Additionally, feedback from physical therapists and patients could be collected to improve the user interface design of the web application, ensuring functionalities align with real-world rehabilitation needs.

ACKNOWLEDGMENTS

This work is co-funded by the European Union through the Erasmus+ project *AiRobo: Artificial Intelligence-based Robotics*, 2023-1-RO01-KA220-HED-000152418.

REFERENCES

Autodesk Inc. (2025). Tinkercad. Online 3D design and modeling platform.

Chiri, A., Giovacchini, F., Vitiello, N., Cattin, E., Roccella, S., Vecchi, F., and Carrozza, M. C. (2009). HAN-DEXOS: Towards an exoskeleton device for the rehabilitation of the hand. In 2009 IEEE/RSJ International Conference on Intelligent Robots and Systems, IROS 2009, pages 1106–1111.

Chirinos, S. and Vela, E. (2021). A Modular Soft Robotic Exoskeleton for Active Hand Rehabilitation after Stroke. In 2021 IEEE Engineering International Research Conference (EIRCON), pages 1–4.

Feigin, V. L., Brainin, M., Norrving, B., Martins, S. O., Pandian, J., Lindsay, P., Grupper, M. F., and Rautalin, I. (2025). World Stroke Organization: Global Stroke Fact Sheet 2025. *International Journal of Stroke*, 20(2):132–144. PMID: 39635884.

- Fiorilla, A., Tsagarakis, N., Nori, F., and Sandini, G. (2009). Design of a 2-Finger Hand Exoskeleton for Finger Stiffness Measurements. *Applied Bionics and Biomechanics*, 30:1–13.
- Hesse, S., Heß, A., Werner C, C., Kabbert, N., and Buschfort, R. (2014). Effect on arm function and cost of robot-assisted group therapy in subacute patients with stroke and a moderately to severely affected arm: a randomized controlled trial. *Clinical rehabilitation*, 28(7):637–647.
- Ho, S., Tong, R. K.-Y., Hu, X., Fung, K., Wei, X., Rong, W., and Susanto, E. (2011). An EMG-driven exoskeleton hand robotic training device on chronic stroke subjects: Task training system for stroke rehabilitation. *IEEE International Conference on Rehabilita*tion Robotics, 2011:5975340.
- Kahn, L. E., Zygman, M. L., Rymer, W. Z., and Reinkensmeyer, D. J. (2006). Robot-assisted reaching exercise promotes arm movement recovery in chronic hemiparetic stroke: a randomized controlled pilot study. *Journal of neuroengineering and rehabilitation*, 3(1):12.
- Masiero, S., Celia, A., Rosati, G., and Armani, M. (2007). Robotic-assisted rehabilitation of the upper limb after acute stroke. Archives of physical medicine and rehabilitation, 88(2):142–149.
- Ridremont, T., Singh, I., Bruzek, B., Jamieson, A., Gu, Y., Merzouki, R., and Wijesundra, M. (2024). Pneumatically Actuated Soft Robotic Hand and Wrist Exoskeleton for Motion Assistance in Rehabilitation. *Actuators*, 13:180.
- Sale, P., Franceschini, M., Mazzoleni, S., Palma, E., Agosti, M., and Posteraro, F. (2014). Effects of upper limb robot-assisted therapy on motor recovery in subacute stroke patients. *Journal of NeuroEngineering and Re-habilitation*, 11(1):104.
- Sandison, M., Phan, K., Casas, R., Nguyen, L., Lum, M., Pergami-Peries, M., and Lum, P. S. (2020). Hand-MATE: Wearable Robotic Hand Exoskeleton and Integrated Android App for At Home Stroke Rehabilitation. In 2020 42nd Annual International Conference of the IEEE Engineering in Medicine & Biology Society (EMBC), pages 4867–4872.
- Selvaraj Mercyshalinie, E. R., Ghadge, A., Ifejika, N., and Tadesse, Y. (2023). NOHAS: A Novel Orthotic Hand Actuated by Servo Motors and Mobile App for Stroke Rehabilitation. *Robotics*, 12:169.
- Takahashi, K., Domen, K., Sakamoto, T., Toshima, M., Otaka, Y., Seto, M., Irie, K., Haga, B., Takebayashi, T., and Hachisuka, K. (2016). Efficacy of Upper Extremity Robotic Therapy in Subacute Poststroke Hemiplegia. Stroke, 47(5):1385–1388.
- Wang, D., Wang, Y., Zi, B., Cao, Z., and Ding, H. (2020). Development of an active and passive finger rehabilitation robot using pneumatic muscle and magnetorheological damper. *Mechanism and Machine Theory*, 147:103762.
- Yap, H. K., Koh, T., Sun, Y., Liang, X., Lim, J., and Yeow, R. C.-H. (2017). A Fully Fabric-Based Bidirectional Soft Robotic Glove for Assistance and Rehabilitation

- of Hand Impaired Patients. *IEEE Robotics and Automation Letters*, PP:1–1.
- Yap, H. K., Lim, J., Nasrallah, F., Low, F.-Z., Cho, J., and Yeow, R. C.-H. (2015). MRC-glove: A fMRI compatible soft robotic glove for hand rehabilitation application. In 2015 IEEE International Conference on Rehabilitation Robotics (ICORR), pages 735–740.
- Zeng, H., Chen, J., Guo, Y., and Tan, S. (2021). Prevalence and Risk Factors for Spasticity After Stroke: A Systematic Review and Meta-Analysis. Frontiers in Neurology, 11:616097.

